

Accumulation of freshwater in the permanent ice zone of the Canada Basin during summer 2008

TONG Jinlu¹, CHEN Min^{1*}, YANG Weifeng^{1, 2}, ZHANG Run¹, PAN Hong¹, ZHENG Minfang¹, QIU Yusheng^{1, 2}, HU Wangjiang¹, ZENG Jian¹

¹ College of Ocean and Earth Sciences, Xiamen University, Xiamen 361102, China

² State Key Laboratory of Marine Environmental Science, Xiamen University, Xiamen 361102, China

Received 27 May 2016; accepted 19 September 2016

©The Chinese Society of Oceanography and Springer-Verlag Berlin Heidelberg 2017

Abstract

A combination of $\delta^{18}\text{O}$ and salinity data was employed to explore the freshwater balance in the Canada Basin in summer 2008. The Arctic river water and Pacific river water were quantitatively distinguished by using different saline end-members. The fractions of total river water, including the Arctic and Pacific river water, were high in the upper 50 m and decreased with depth as well as increasing latitude. In contrast, the fraction of Pacific river water increased gradually with depth but decreased toward north. The inventory of total river water in the Canada Basin was higher than other arctic seas, indicating that Canada Basin was a main storage region for river water in the Arctic Ocean. The fraction of Arctic river water was higher than Pacific river water in the upper 50 m while the opposite was true below 50 m. As a result, the inventories of Pacific river water were higher than those of Arctic river water, demonstrating that the Pacific inflow through the Bering Strait is the main source of freshwater in the Canada Basin. Both the river water and sea-ice melted water in the permanent ice zone were more abundant than those in the region with sea-ice just melted. The fractions of total river water, Arctic river water, Pacific river water increased northward to the north of 82°N , indicating an additional source of river water in the permanent ice zone of the northern Canada Basin. A possible reason for the extra river water in the permanent ice zone is the lateral advection of shelf waters by the Trans-Polar Drift. The penetration depth of sea-ice melted waters was less than 30 m in the southern Canada Basin, while it extended to 125 m in the northern Canada Basin. The inventory of sea-ice melted water suggested that sea-ice melted waters were also accumulated in the permanent ice zone, attributing to the trap of earlier melted waters in the permanent ice zone via the Beaufort Gyre.

Key words: ^{18}O , freshwater, river water, sea ice melted water, Canada Basin

Citation: Tong Jinlu, Chen Min, Yang Weifeng, Zhang Run, Pan Hong, Zheng Minfang, Qiu Yusheng, Hu Wangjiang, Zeng Jian. 2017. Accumulation of freshwater in the permanent ice zone of the Canada Basin during summer 2008. *Acta Oceanologica Sinica*, 36(8): 101–108, doi: 10.1007/s13131-017-1023-1

1 Introduction

Freshwater plays a dynamic role in global climate by affecting air-ice-ocean heat exchange in the Arctic Ocean (Carmack, 2000). It maintains strong stratification that inhibits heat transfer from deep ocean to the surface, and consequently has a dramatic effect on sea ice cover, even the Arctic climate system (Shimada et al., 2006). Freshwater affects not only circulations in the Arctic Ocean but also affects convective processes in the North Atlantic (Aagaard and Carmack, 1989; Proshutinsky et al., 2002). In the Arctic Ocean, the largest amount of freshwater, including sea-ice melted water, river water and low-salinity Pacific water flowed through the Bering Strait (Steele et al., 2004), is stored in the Beaufort Gyre (BG) in the Canadian Basin. The quantification of freshwater components, including their source, distribution and pathway, is crucial for understanding the fate of pollutants, nutrients, and marine processes in the Arctic Ocean (Cai et al., 2010; Yamamoto-Kawai et al., 2006, 2008).

$\delta^{18}\text{O}$ and salinity (S) are usefully conservative tracers for calculating fractions of river water and sea-ice melted water, as river water is highly depleted in $\delta^{18}\text{O}$ relative to sea-ice melted water

and saline water. Since its first successful application in the Fram Strait and Eurasian Basin (Östlund and Hut, 1984), $\delta^{18}\text{O}$ - S method has been widely used in the Arctic seas. One of the most important findings is that a great amount of river runoff is stored in the interior Arctic Ocean, especially in the southern Canada Basin (Macdonald et al., 2002; Chen et al., 2003; Yamamoto-Kawai et al., 2008; Jones et al., 2008; Newton et al., 2013). It has been proposed that the variation in freshwater accumulated in the Canada Basin is generally modulated by strength of the wind-driven Beaufort Gyre (Giles et al., 2012). A significant amount of freshwater is accumulated during anticyclonic regime and released to the North Atlantic during cyclonic regime (Proshutinsky et al., 2002, 2009). More recently, Morison et al. (2012) suggested that the freshening of the Canada Basin during 1990s–2008 should be ascribed to the runoff pathway variation modulated by the Arctic Oscillation (AO) or the changes of wind-stress curl. Based on the $\delta^{18}\text{O}$ and other geochemical evidences, it has been confirmed that the Pacific inflow is the main source of freshwater below ~ 50 m in the Canada Basin (Jones et al., 2008; Yamamoto-Kawai et al., 2008). On the other hand, the southern

Foundation item: The Chinese Polar Environment Comprehensive Investigation & Assessment Program under contract Nos CHINARE2017-03-04-03 and CHINARE2017-04-03-05; the Natural Science Foundation of China under contract No. 41125020.

*Corresponding author, E-mail: mchen@xmu.edu.cn

Canada Basin was reported to be a significant net producer of sea ice (Melling and Moore, 1995; Chen et al., 2003), as well as the shelf and slope (Bauch et al., 1995, 2011; Macdonald et al., 1995; Melling and Moore, 1995; Anderson et al., 2013). Sea ice formation was accompanied by the formation of the upper halocline water in the Canada Basin (Bauch et al., 2011; Anderson et al., 2013). Macdonald et al. (2002) reported net ice formation from the continental margin to 200 km offshore, but net sea-ice melted waters under permanent pack in the southern Canada Basin. Yamamoto-Kawai et al. (2005) found that net ice melting occurred along the surface flow of water from the Pacific and the Atlantic, while net ice formation resided in the central Arctic Ocean. Because of the perennial sea ice cover in the northern Canada Basin, the freshwater source and budget have been rarely studied. The purpose of this study is to investigate the source of freshwater in the Canada Basin, especially freshwater accumulation in the permanent ice zone, which is covered by sea ice all year.

In this study, $\delta^{18}\text{O}$ -salinity approach under two different saline end-members was used to determine the fractions of total river water, Arctic river water, Pacific river water, and sea-ice melted water. The spatial distributions of total river water, Arctic river water, Pacific river water and sea-ice melted water were examined to reveal their source and pathways in the Canada Basin, especially in the northern Canada Basin. Lastly, the mechanism of accumulation for freshwater in the permanent ice zone was discussed.

2 Materials and methods

2.1 Sampling

Seawater samples were collected using 10 L Niskin bottles mounted on a rosette together with SBE-911^{plus} conductivity-temperature-depth (CTD) sensors in the western Arctic Ocean, aboard the R/V *Xuelong* during August 10–29, 2008. A total of 18 stations were surveyed, covering a region among 71.9–85.4°N, 154.7–143.5°W. Most stations were located in the Canada Basin with water depths greater than 2 000 m, and two stations (S22, S23) were situated on the Beaufort slope (Fig. 1). The north-south section begins north of Barrow, Alaska, at 71.9°N, 154.7°W, in approximately 100 m water depth over the Alaskan continental shelf, and ends off the Alpha-Mendeleyev Ridge (AMR), at 85.4°N, 147.5°W (Fig. 1). Seawater samples for ^{18}O measurement were filled bubble-free into 50 mL polypropylene bottles and sealed until analysis in land laboratory.

2.2 Seawater ^{18}O analysis

Once return, seawater ^{18}O was determined by $\text{CO}_2\text{-H}_2\text{O}$ equilibration method (Horita et al., 1989; Bourg et al., 2001). Briefly, ^{18}O in seawater was equilibrated with CO_2 at 25°C for 24 h, and detected with a Finnigan Delta^{plus} XP isotopic ratio mass spectrometer. A series of working standards (with $\delta^{18}\text{O}$ values of -8.71‰, -5.63‰, 0.34‰, 0.39‰, respectively) pre-calibrated against Vienna Standard Mean Ocean Water (VSMOW) were used for determining ^{18}O abundance. These standards were inserted during measurement at an interval of about ten samples. Each sample was measured repeatedly for ten times.

Stable isotopic composition of oxygen in seawater was reported as delta value (δ) given in per mill:

$$\delta^{18}\text{O} = \left[\frac{(^{18}\text{O}/^{16}\text{O})_{\text{sample}}}{(^{18}\text{O}/^{16}\text{O})_{\text{VSMOW}}} - 1 \right] \times 1000, \quad (1)$$

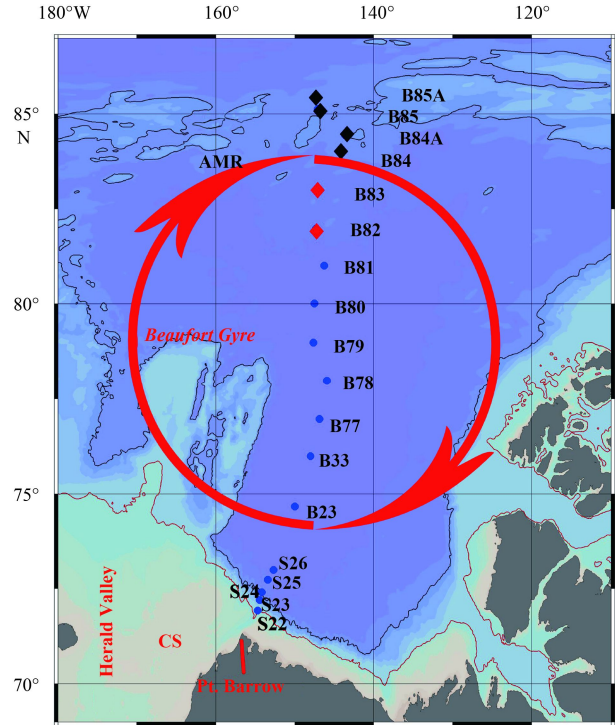


Fig. 1. Sampling locations for seawater ^{18}O measurements in the Canada Basin during summer 2008. AMR represents Alpha-Mendeleyev Ridge, and CS Chukchi Sea. The area of southern Canada Basin is outlined by blue dot, while the area of northern Canada Basin is outlined by diamond. The red and black diamonds represent stations in the region with sea-ice just melted and in the permanent ice zone, respectively.

where the subscript “sample” and “VSMOW” denoted the measured seawater and the Vienna Standard Mean Ocean Water, respectively. The reproducibility for seawater $\delta^{18}\text{O}$ measurement was within 0.025‰.

2.3 Freshwater component calculation

The fractions (%) of each freshwater component can be derived from mass balance calculation as follows:

$$f_s + f_r + f_{\text{SIM}} = 1, \quad (2)$$

$$f_s \times S_s + f_r \times S_r + f_{\text{SIM}} \times S_{\text{SIM}} = S_M, \quad (3)$$

$$f_s \times \delta^{18}\text{O}_s + f_r \times \delta^{18}\text{O}_r + f_{\text{SIM}} \times \delta^{18}\text{O}_{\text{SIM}} = \delta^{18}\text{O}_M, \quad (4)$$

where f_s, f_r, f_{SIM} are fractions (%) of the saline water, river water and sea-ice melted water, respectively. S_M and $\delta^{18}\text{O}_M$ represent the measured salinity and $\delta^{18}\text{O}$ values in seawater sample respectively. The inventories of river water (I_r , m) and sea-ice melted water (I_{SIM} , m) were calculated from a trapezoidal integration over the depth at which the river water fraction declined to zero.

The end-member values of $\delta^{18}\text{O}$ and salinity assessed for the Atlantic Water, river water and sea-ice melted water were listed in Table 1. The values of $\delta^{18}\text{O}$ and salinity for the river water were adopted as -20‰ and 0, respectively (Cooper et al., 2005; Yamamoto-Kawai et al., 2008). As for sea-ice melted water, values -2.0‰ and 4 were chosen as the end-member values of $\delta^{18}\text{O}$

Table 1. The end-member values used for mass balance calculation

End-member	$^{18}\text{O}/\text{‰}$	Salinity	Reference
Atlantic Water	0.30	35.00	Ekurzel et al. (2001)
Winter Bering Sea Water	-1.10	33.10	Macdonald et al. (2002)
River water	-20.00	0	Cooper et al. (2005)
Sea-ice melted water	-2.00	4.00	Macdonald et al. (2002)

and salinity (Macdonald et al., 2002). In order to discern the contribution of Arctic river water and Pacific river water, both the winter Bering Sea Water and the Atlantic Water were assigned as the end-member saline water in this study. When the Atlantic Water (AW, $S=35$, $\delta^{18}\text{O}=0.3\text{‰}$; Ekurzel et al., 2001) was adopted as the end-member, the fraction of total river water (f_r^{total}) can be calculated, representing the sum of the Arctic river water and the Pacific river water. When the winter Bering Sea Water (wBSW, $S=33.1$, $\delta^{18}\text{O}=-1.1\text{‰}$; Macdonald et al., 2002) was adopted, the calculated fraction of river water (f_r^{Arctic}) represents the contribution solely from the Arctic river runoff. The difference between f_r^{total} and f_r^{Arctic} stands for the contribution of Pacific river water (f_r^{Pacific}). In this calculation, the calculated fractions of river water will be biased when the end-member value of $\delta^{18}\text{O}$ in the Arctic rivers is not equal to that of the Pacific rivers. Fortunately, the end-member value of $\delta^{18}\text{O}$ in the Arctic rivers was not significantly different to that of the Pacific rivers. The end-member $\delta^{18}\text{O}$ values in the Arctic rivers were reported as $(-20\pm 2)\text{‰}$ (Östlund and Hut, 1984; Bauch et al., 1995, 2011; Ekurzel et al., 2001; Macdonald et al., 2002; Cooper et al., 2005, 2008; Yamamoto-Kawai et al., 2008, 2009), while those of the Pacific rivers (most from Yukon River) ranged from -17‰ to -23‰ with an average of $(-19.5\pm 4)\text{‰}$ (Coplen and Kendall, 2000; Grebmeier et al., 1990; Cooper et al., 1997, 2005). The sensitivity analysis indicated that uncertainties of the calculated fractions of the river water and sea-ice melted water were mostly sensitive to the end-member value of $\delta^{18}\text{O}$ for the river water. However, the calculated fractions of the river water and sea-ice melted water were biased only less than 2% when the end-member value of $\delta^{18}\text{O}$ varied from -20‰ to -19.5‰ (Tong et al., 2014; Pan et al., 2015).

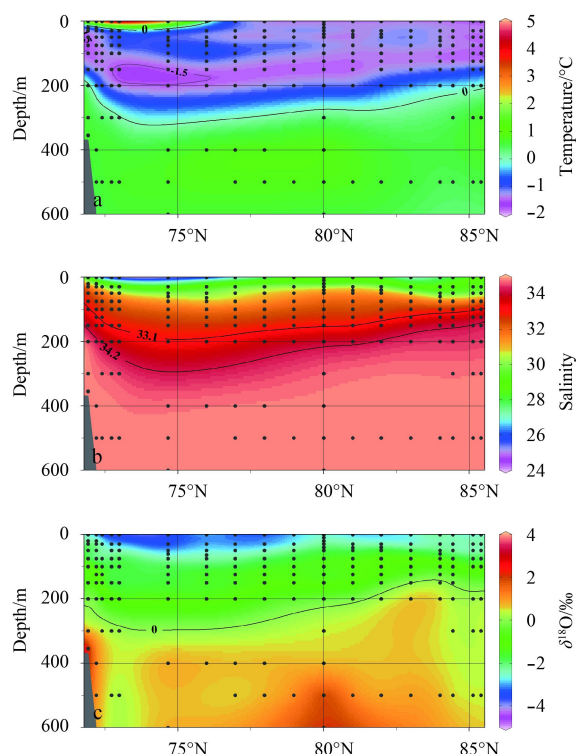
3 Results

3.1 Temperature

Temperature in the upper 200 m along the transect showed clearly a south-north decreasing pattern (Fig. 2a). To the south of 82°N , temperature ranged from -1.51°C to -0.66°C at depth of 50–150 m, while temperature was relatively low (-1.51°C to -1.13°C) in north of 82°N . The depth of the coldest water in the southern basin (~ 200 m) was deeper than that in the northern basin (~ 150 m). Temperature at depth of 300–600 m was greater than 0.3°C with little variability, probably indicating the warming of the Arctic Intermediate Water (Carmack et al., 1995; Zhao et al., 2005).

3.2 Salinity

Salinity in the upper 50 m to south of 82°N (24.8–31.7) was lower than those to the north of 82°N (24.8–32.4) (Fig. 2b), implying the influence of sea-ice melted water and river water. Salinity increased northward in the southern region while slightly decreased with increasing latitude in the northern basin. Salinity increased with depth to about 34.2 at 200–300 m. Two haloclines were observed at 50–150 m and 200–300 m, corresponding to the Upper Halocline Water (core salinity 33.1) and the Lower Halo-

**Fig. 2.** Distributions of temperature (a), salinity (b), and $\delta^{18}\text{O}$ (c) in the upper 600 m water column in the Canada Basin.

cline Water (core salinity 34.2) (Jones and Anderson, 1986; Rudels et al., 1996), respectively. The waters with salinity higher than 34.2 below 200 m was called the Arctic Intermediate Water (Jones et al., 1998; Chen et al., 2003; Shi et al., 2005). Salinity at depth of 300–600 m ranged from 34.6 to 34.9 along the transect.

3.3 $\delta^{18}\text{O}$

Surface $\delta^{18}\text{O}$ values ranged from -4.01‰ to -1.04‰ with an average of -2.98‰ , showing an increase from 71.9°N to 82°N and then a slightly decrease northward (Fig. 2c). In the upper 200 m water column, $\delta^{18}\text{O}$ values generally increased downward but with a more rapid increase in north of 82°N . The lowest $\delta^{18}\text{O}$ values (-4.01‰ to -3.07‰) were observed in surface water. The $\delta^{18}\text{O}$ values to the south of 82°N (-4.01‰ to -1.68‰) were lower than those to the north of 82°N (-2.88 to -1.59‰) in the upper 50 m water column. $\delta^{18}\text{O}$ values below 150 m reached around 0.3‰ in the north of 82°N , illustrating the characteristic of the Atlantic Water, but this signal was not observed until 200 m in south of 82°N . Obviously, the isoline with $\delta^{18}\text{O}$ value of zero was shoaled toward north, indicating much stronger influence of freshwater in the southern Canada basin.

$\delta^{18}\text{O}$ values in the upper 50 m water column mostly lie to the left of the two end-member conservative mixing line of Pacific Water and river water (Fig. 3), suggesting a notable influence of the sea-ice melted water. In contrast, $\delta^{18}\text{O}$ values at depths of 50–200 m (with salinities of about 33.1) stand to the right of the mixing line (Fig. 3), indicating an effect of brine water. The freezing and melting of sea ice resulted in a large variability in salinity but relatively small variability in seawater $\delta^{18}\text{O}$ values. The fractionation factor of oxygen isotopes during either freezing or melting of sea ice was generally within 2‰ (Melling and Moore, 1995; Eicken et al., 2002; Macdonald et al., 2002; Pfirman et al., 2004). Most of seawater $\delta^{18}\text{O}$ at depths of 200–600 m were greater than

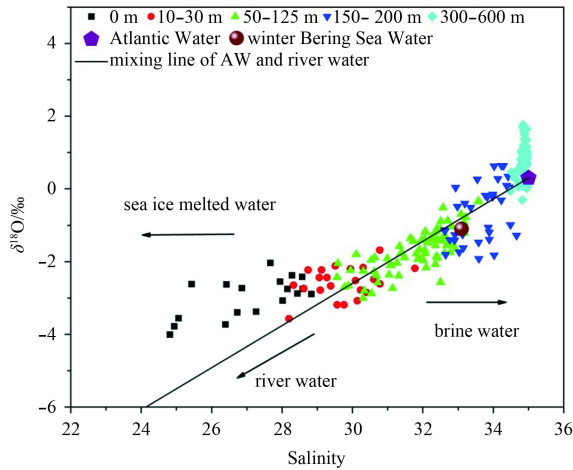


Fig. 3. Relationship between $\delta^{18}\text{O}$ and salinity in the Canada Basin. The arrows represent mixing with meteoric water, sea-ice melted water and brine, respectively.

zero and close to the characteristic value (0.3‰) of the Atlantic Water (Ekurzel et al., 2001). Interestingly, $\delta^{18}\text{O}$ value of the winter Bering Sea Water fall on the conservative mixing line of the Atlantic Water and river water (Fig. 3), suggesting that the winter Bering Sea Water can be expressed as a linear mixture of the Atlantic Water and river water on the $\delta^{18}\text{O}$ -S diagram but with no contribution of Arctic river water. We thus suggest that water mass in our study area can be regarded as a mixture of the river water (including Arctic river water and Pacific river water), sea-ice melted water and Atlantic Water.

3.4 Components of river water

The fractions of total river water (f_r^{total}) and Arctic river water (f_r^{Arctic}) both decreased with depth and increasing latitude, but slightly increased northward to north of 82°N (Figs 4a and b). The largest f_r^{total} (17.4%–20.1%) and f_r^{Arctic} (11.7%–14.8%) were both observed in surface waters in the southern Canada Basin. Two contour lines of f_r^{total} (8% and 0%) both shoaled toward north, and showed different patterns at the boundary of 82°N as well as f_r^{Arctic} (5% and 0%). To south of 82°N, f_r^{total} decreased with depth from 20.1% in surface water to 0% at about 300 m. f_r^{Arctic} also decreased with depth from 14.8% in surface water to 0% at about 200 m. The f_r^{total} was almost zero below 300 m, while f_r^{Arctic} was close to zero below 200 m, indicating the penetration depth of the total river water (300 m) was deeper than the Arctic river water (200 m) in the southern Canada Basin. f_r^{total} and f_r^{Arctic} showed an opposite spatial characteristic to the north of 82°N with a slightly increase with increasing latitude. The depth of two contour lines of f_r^{total} (8% and 0%) increased northward, corresponding to an increased penetration depth of total river water from ~200 m to ~300 m. Similarly, the penetration depth of Arctic river water was also increased northward from ~100 m to ~125 m. Thus, the total river water and Arctic river water were more abundant toward high latitudes in the northern Canada Basin.

The fractions of Pacific river water (f_r^{Pacific}) gradually increased with depth till the lower halocline, and then sharply decreased to zero below (Fig. 4c). The f_r^{Pacific} was lower than f_r^{Arctic} at depth of 0–50 m, while the opposite was true at deeper layers (Figs 4b and c), indicating that the Pacific inflow was the main source of river water below 50 m depth in the Canada Basin. The distribution of f_r^{Pacific} also showed different characteristics at the

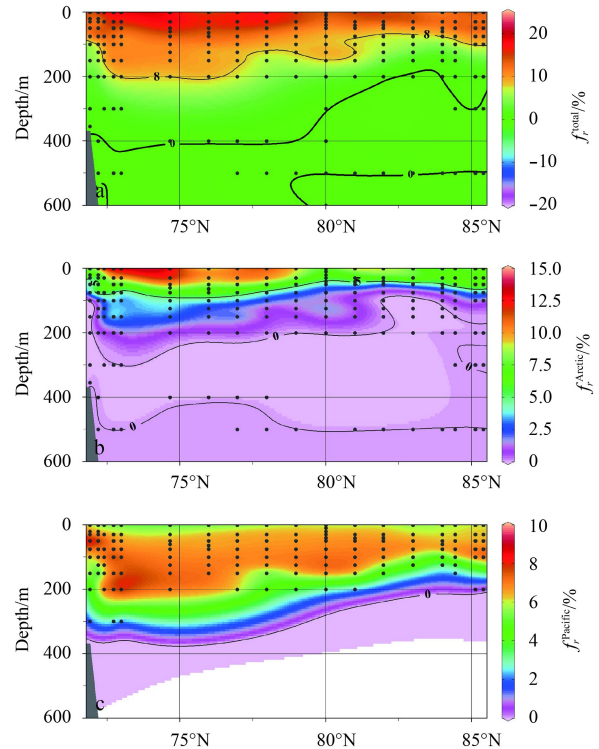


Fig. 4. Distribution of the fraction (%) of total river water (f_r^{total} , a), Arctic river water (f_r^{Arctic} , b), Pacific river water (f_r^{Pacific} , c) along the N-S transect.

boundary of 82°N. The f_r^{Pacific} values increased with depth from 5.2% in surface water to 8.9% at about 200 m, and then sharply decreased to 0%–3.2% at depth of 300 m in the southern Canada Basin. Below 300 m, there was no Pacific river water, indicating that the penetration depth to the south of 82°N was about 300 m. Comparably, f_r^{Pacific} increased slightly with depth from 5.6% in surface water to 7.1% at about 100 m, and then decreased rapidly to 0%–3.8% at 125–200 m to the north of 82°N. Obviously, the penetration depth of f_r^{Pacific} in the northern Canada Basin was shallow to 200 m.

The inventories of three river water components (I_r^{total} , I_r^{Arctic} and I_r^{Pacific}) in the water column were listed in Table 2. Because I_r^{total} represented the total river water imported into the Canada Basin, it was higher than I_r^{Pacific} . I_r^{total} , I_r^{Arctic} and I_r^{Pacific} were (19.1±4.0) m, (8.3±2.8) m and (10.8±2.1) m, respectively, in the southern Canada Basin. By comparison, such values decreased to (10.3±1.7) m, (4.5±0.9) m and (5.9±1.0) m, respectively, in the northern Canada Basin. It is clearly shown that more abundant river water was stored in the southern Canada Basin, probably due to the Ekman convergence of Beaufort Gyre (Proshutinsky et al., 2002, 2009).

The inventory of total river water in the Canada Basin was higher than previous estimates in the Makarov Basin (11.5 m), the Amundsen Basin (9.6 m) and the Nansen Basin (2.9 m) (Bauch et al., 1995), but close to that in the Canadian Basin (13 m; Bauch et al., 1995), indicating that the Canada Basin was a main storage region of river water in the Arctic Ocean, despite most of the river discharge was located in the eastern Arctic. This discrepancy may be related to the change of atmospheric pressure fields to cyclonicity (Proshutinsky and Johnson, 1997; Thompson and Wallace, 1998), and the resultant altered pathway of major Russian rivers spreading onto the East Siberian

Table 2. The fractions and inventories of total river water, Arctic river water, Pacific river water and sea-ice melted water in the southern and northern Canada Basin

Region	Freshwater component	Fraction/%		Inventory/m	
		Range	Average	Range	Average
Southern basin	total river water	0–20.1	10.8±4.5	14.9–26.0	19.1±4.0
	Arctic river water	0–14.8	4.6±3.9	4.7–12.7	8.3±2.8
	Pacific river water	0–8.9	6.3±1.4	6.9–13.5	10.8±2.1
	sea-ice melted water	–9.1–16.8	–0.8±4.5	–9.1–3.3	–3.1±3.6
Northern basin	total river water	0–15.2	8.2±4.8	7.9–12.4	10.3±1.7
	Arctic river water	0–9.1	4.2±3.0	3.3–5.9	4.5±0.9
	Pacific river water	0–7.1	5.8±1.4	4.6–6.6	5.9±1.0
	sea-ice melted water	–3.7–12.2	2.1±3.2	1.2–8.5	4.0±2.8

Shelf instead of flowing directly into the Trans-Polar Drift (TPD) (Semiletov et al., 2000; Ekwurzel et al., 2001; Guay et al., 2001; Johnson and Polyakov, 2001). Such forcing would undoubtedly promote the accumulation of river water in the Canada Basin (Proshutinsky et al., 2002; Shimada et al., 2006).

3.5 Component of sea-ice melted water

$f_{SIM-wBSW}$ was a little higher than f_{SIM-AW} (1.5%–1.9%), due to that the mixing line of RR and wBSW slightly lied to the right of the mixing line of RR and AW (Fig. 3). However, $f_{SIM-wBSW}$ and f_{SIM-AW} showed the same spatial pattern in the Canada Basin (Figs 5a and b), and thus only the f_{SIM-AW} was used for discussion in this study.

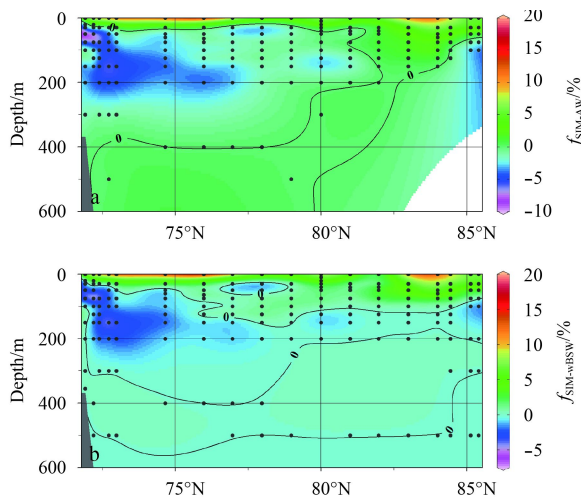


Fig. 5. Distributions of f_{SIM-AW} (a), $f_{SIM-wBSW}$ (b) along the N-S transect.

f_{SIM-AW} showed different patterns with the boundary of 82°N (Fig. 5a). The maximum f_{SIM-AW} was observed at depth of 0 m (2.5%–16.8%), indicating an intense sea ice melting in surface water. f_{SIM-AW} decreased rapidly with increasing depth (–3.9%–16.8%) with the penetration depth less than 30 m in the southern Canada Basin. By contrast, the penetration depth of sea-ice melted water (0.2%–12.2%) was more than 50 m to the north of 82°N. A weak signal of sea-ice melted water (~1%) was even observed at depth of 100–125 m at Stas B82, B83 and B84, reflecting abundant sea-ice melted waters accumulated in the northern Canada Basin.

The minimum core of f_{SIM-AW} extended northward from the depth of 50 m on the slope to the depth of 200 m at 82°N (Fig. 5a), corresponding to the maximum layer of $f_r^{Pacific}$ (Fig. 4c). The neg-

ative f_{SIM-AW} at these layers indicated that saline brines released during sea ice formation involved in the formation of Upper Halocline Layer in the Canada Basin, similar to the results of previous sampling campaign during summer 1999 (Chen et al., 2003). Interestingly, negative values of f_{SIM-AW} were also found below 50 m at the three high-latitude basin stations (B84A, B85 and B85A; Fig. 5a), indicating the influence of brines advected from shelf regions. Similarly, Bauch et al. (2011) found a pronounced layer influenced by brines released during sea-ice formation is present at depths of 30–50 m over the Lomonosov Ridge, which was attributed to advection from shelf regions.

4 Discussion

4.1 Pacific inflow is a major source of freshwater in the Canada Basin

$I_r^{Pacific}$ is designated by “Pacific river water” which represented the river runoff contributed by Pacific inflow. The $I_r^{Pacific}$ ranged from 4.6 m to 13.5 m, with an average of (8.4±2.8) m in the Canada Basin, while the I_r^{Arctic} was 3.3–12.7 m, with an average of (6.7±2.8) m. In addition, the inventory of Pacific river water was always higher than Arctic river water, except for Stas S24 and S25 (Fig. 6). The contribution of Pacific river water to total river water

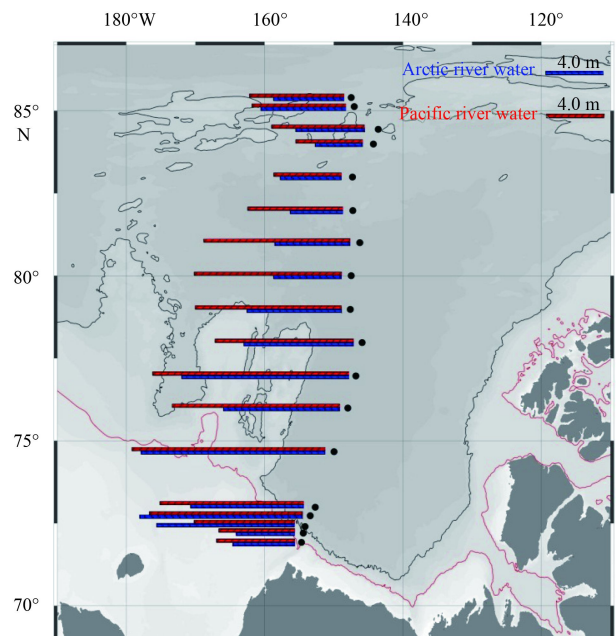


Fig. 6. Inventory of Arctic river water (blue) and Pacific river water (red) along the N-S transect.

($I_r^{\text{Pacific}}/I_r^{\text{total}}$) ranged from 51.2% to 68.3% except for Stas S24 and S25 (42.2% and 48.5%) in the Canada Basin. They both demonstrated that the Pacific inflow was the major source of river water in the Canada Basin. Considering the averaged inventory of sea-ice melted water was only -0.8 m, it thus confirms that the Pacific river water was the major contributor of freshwater in the Canada Basin in summer 2008. Aagaard and Carmack (1989) estimated the freshwater flux through the Bering Strait as $1\,670\text{ km}^3/\text{a}$ based on an annual velocity of water transport (0.8 Sv) and salinity (32.5), which was about $1/3$ of the total freshwater input to the Arctic. Woodgate and Aagaard (2005) revised the freshwater flux through the Bering Strait from $1\,670\text{ km}^3/\text{a}$ to $2\,500\text{ km}^3/\text{a}$, implying more freshwater was transported to the Arctic Ocean by the Pacific inflow. Woodgate et al. (2006) reported that the increase of Pacific river water ($\sim 800\text{ km}^3$) in the Canada Basin from 2001 to 2004 was about $1/4$ of annual Arctic river runoff. Besides, the mooring data indicated that the Bering Strait throughflow increased $\sim 50\%$ from 2001 ($\sim 0.7\text{ Sv}$) to 2011 ($\sim 1.1\text{ Sv}$), and the freshwater flux variability exceeds variability in other Arctic freshwater sources (Woodgate et al., 2012). Obviously, the Pacific inflow is a major source of freshwater in the Canada Basin.

4.2 Accumulation of river water and sea-ice melted water in permanent ice zone

As described in Section 3.4, f_r (f_r^{total} , f_r^{Arctic} and f_r^{Pacific}) slightly increased toward the north pole from 82°N and the penetration depth of f_r was deeper in the northern Canada Basin, indicating that river water, including the Arctic river water and the Pacific river water, was more abundant in the permanent ice zone than those in the region with sea-ice just melted in the northern Canada Basin. On the basis of geographic position, stations to the north of 84°N (B84, B84A, B85, and B85A) were located around the Alpha-Mendeleyev Ridge (Fig. 1), the I_r^{total} , I_r^{Arctic} and I_r^{Pacific} at these stations were $7.9\text{--}10.2\text{ m}$, $3.3\text{--}4.3\text{ m}$ and $4.6\text{--}6.6\text{ m}$, with an average of $(9.0\pm 1.2)\text{ m}$, $(3.7\pm 0.5)\text{ m}$ and $(5.3\pm 1.1)\text{ m}$, respectively (Fig. 6). By comparison, I_r^{total} , I_r^{Arctic} and I_r^{Pacific} at Stas B82 and B83 were $11.2\text{--}12.4\text{ m}$, $4.8\text{--}5.9\text{ m}$ and $6.4\text{--}6.5\text{ m}$, with an average of $(11.7\pm 0.6)\text{ m}$, $(5.2\pm 0.6)\text{ m}$ and $(6.5\pm 0.1)\text{ m}$, respectively (Fig. 6). Obviously, I_r^{total} , I_r^{Arctic} and I_r^{Pacific} to north of 84°N increased by 2.7 m , 1.5 m and 1.2 m , respectively, similar to observation by Newton et al. (2013). Both the increase of I_r^{Arctic} and I_r^{Pacific} to the north of 84°N suggested accumulation of the Arctic river water and Pacific river water in the permanent ice zone in the northern Canada Basin.

Two mechanisms may be responsible for the accumulation of I_r^{Arctic} and I_r^{Pacific} in the northern Canada Basin. First, the higher Arctic river water around the Alpha-Mendeleyev Ridge may result from topographically trapped river waters from the Trans-Polar Drift (TPD) during their transport from the Siberia to the Fram Strait. TPD originated from the continental shelves containing abundant river water (Newton et al., 2008). The flow of TPD was driven by the steric height gradient between the Siberian-Alaskan shelves and the North Atlantic, and the prevailing wind stress between the Canadian and Eurasian Basins. Less energy input is required at these features to balance vorticity changes as the thickness of isopycnal layers increases, and thus the trans-Arctic transport tends to follow the flanks of the ridges as it crosses the central basin (Holloway and Wang, 2009; Newton et al., 2008). The topographically trapped plumes of runoff-rich shelf waters will result in the accumulation of river water over the Alpha-Mendeleyev Ridge. Previous studies suggested that one branch of the Pacific inflow was incorporated into TPD at the north of Herald Valley (Steele et al., 2004). This branch provided the addition-

al Pacific river water for the northern Canada Basin. Second, the AO index increased from -0.38 to 0.18 during 2005–2008 (data from NOAA), indicating that surface circulation became more anticyclonic in the Arctic Ocean. This change will result in more coastal water to be carried across shelf to the eastern Makarov Basin and Chukchi borderland regions, and further incorporated into the BG (Morison et al., 2012). Meanwhile, a branch of the Pacific inflow located at northwest of Herald Valley would incorporate into the BG (Pickart et al., 2010). The modified waters flowing along the Alpha-Mendeleyev Ridge increased the I_r^{Arctic} and I_r^{Pacific} in the northern Canada Basin.

The inventories of sea-ice melted water ($I_{\text{SIM-AW}}$) ranged from -9.1 m to 8.5 m , with an average of -0.7 m in the Canada Basin (Fig. 7), which was higher than previous reported values (Macdonald et al., 2002; Chen et al., 2003; Yamamoto-Kawai et al., 2008; Newton et al., 2013). It seemed that the sea-ice melted water in the Canada Basin increased over the past few years, comparable to the observation by Yamamoto-Kawai et al. (2009). To south of 82°N , most $I_{\text{SIM-AW}}$ values were negative except at Sta. B33, indicating a net ice formation in the southern Canada Basin. Values of $I_{\text{SIM-AW}}$ were more negative at Stas S22, S24 and S25 (Fig. 7), suggesting the Beaufort slope is a major region for sea ice formation, which was consistent with previous results (Macdonald et al., 2002; Bauch et al., 2005). Surprisingly, inventory of sea-ice melted water at Sta. B33 was as large as 3.3 m , showing a significant sea ice melting. The penetration depth of sea-ice melted water at this station (50 m) was also deeper than those in the southern Canada Basin (30 m) (Fig. 5). However, the reason for significant sea ice melting at Sta. B33 was not clear and further studies are needed.

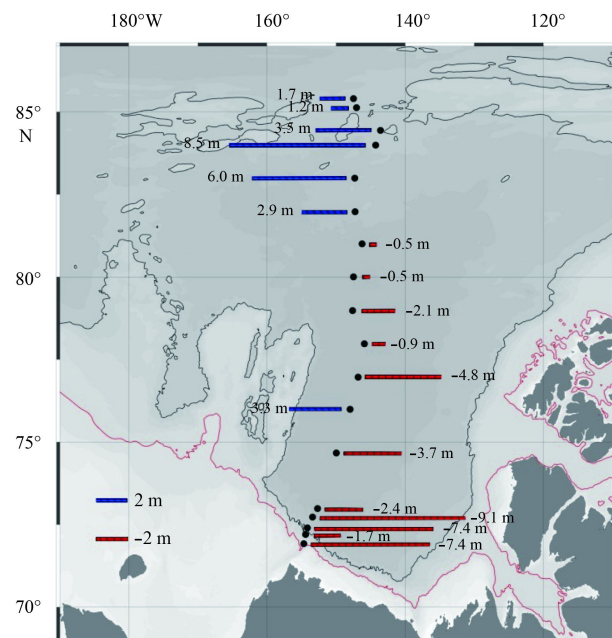


Fig. 7. Inventory of sea-ice melted water along the N-S transect.

The inventory of sea-ice melted water to the north of 82°N ($(4.0\pm 2.8)\text{ m}$) was much higher than those in the southern Canada Basin ($-(3.1\pm 3.6)\text{ m}$, Fig. 7), indicating that a large quantity of sea-ice melted water accumulated in the permanent ice zone during our investigation. This phenomenon was similar to previous observation in the southern Canada Basin (Macdonald et al., 2002; Tong et al., 2014), although the locations of sea ice

melted water accumulation shifted northward. The accumulation of sea ice melted water in the high latitude regions resulted in increase of the penetration depth of sea-ice melted water to more than 50 m in the permanent ice zone (Fig. 5).

It should be noted that the accumulation of sea ice melted water in the permanent ice zone observed during our sampling was contrary to the expectation that more sea-ice melted water would be retained in the southern Canada Basin, due to the earlier melting. We suggest that the lateral transportation of sea-ice melted water could be responsible for this. The sea-ice melted waters were easily suffered from wind fields and surface currents due to their shallow penetration depth. The penetration depths to the south of 82°N were less than 30 m. The early ice melted waters were transported and accumulated in the permanent ice zone by the anti-cyclonic Beaufort Gyre. A marked decline of sea ice in the Canada Basin over 2007 and 2008 (Perovich et al., 2011) will promote surface currents to transport the sea-ice melted waters to the high latitude regions. On the other hand, the presence of pack ice in the permanent ice zone will weaken the surface currents, and keep sea-ice melted waters reserved. Besides advection of the sea ice melted water, the melt pond or polynya existed widely in the high latitude regions may provide an additional effect. The open water in the melt pond or polynya could receive more solar radiation and promote the melting of sea ice.

5 Conclusions

The freshwater components in the Canada Basin during 2008 summer were quantified by $\delta^{18}\text{O}$ and salinity mass balance. The fractions of total river water and Arctic river water decreased with depth and latitude, while the fraction of Pacific river water increased with depth and decreased with latitude. The fractions of Pacific river water were higher than those of Arctic river water below 50 m. As a result, the inventories of Pacific river water were higher than those of Arctic river water in the Canada Basin. This demonstrated that the Pacific inflow through the Bering Strait is a main source of freshwater in the Canada Basin. The river water and sea ice melted water were abnormally accumulated to the north of 82°N in the Canada Basin. The lateral transport of freshwater was proposed to explain this phenomenon. Relatively high river water in the permanent ice zone, including Arctic river water and Pacific river water, was attributed to shelf waters trapped by Trans-Polar Drift or surface circulation. The accumulation of sea-ice melted waters in the permanent ice zone was attributed to the trap of the earlier melted waters by the enhanced Beaufort Gyre. The accumulation of freshwater in the permanent ice zone would profoundly exert influence on biogeochemistry in the Arctic Ocean, thus further studies are undoubtedly necessary to better understand its effects.

References

- Aagaard K, Carmack E C. 1989. The role of sea ice and other fresh water in the Arctic circulation. *J Geophys Res*, 94(C10): 14485–14498
- Anderson L G, Andersson P S, Björk G, et al. 2013. Source and formation of the upper halocline of the Arctic Ocean. *J Geophys Res*, 118(1): 410–421
- Bauch D, Erlenkeuser H, Andersen N. 2005. Water mass processes on Arctic shelves as revealed from $\delta^{18}\text{O}$ of H_2O . *Glob Planet Change*, 48(1–3): 165–174
- Bauch D, Schlosser P, Fairbanks R G. 1995. Freshwater balance and the sources of deep and bottom waters in the Arctic Ocean inferred from the distribution of H_2^{18}O . *Prog Oceanogr*, 35(1): 53–80
- Bauch D, van der Loeff M R, Andersen N, et al. 2011. Origin of freshwater and polynya water in the Arctic Ocean halocline in summer 2007. *Prog Oceanogr*, 91(4): 482–495
- Bourg C, Stievenard M, Jouzel J. 2001. Hydrogen and oxygen isotopic composition of aqueous salt solutions by gas-water equilibration method. *Chem Geol*, 173(4): 331–337
- Cai Weijun, Chen Liqi, Chen Baoshan, et al. 2010. Decrease in the CO_2 uptake capacity in an ice-free Arctic Ocean Basin. *Science*, 329(5991): 556–559
- Carmack E C, Macdonald R W, Perkin R G, et al. 1995. Evidence for warming of Atlantic water in the Southern Canadian Basin of the Arctic Ocean: results from the Larsen-93 Expedition. *Geophys Res Lett*, 22(9): 1061–1064
- Carmack E C. 2000. The Arctic Ocean's freshwater budget: sources, storage and export. In: Lewis E L, Jones E P, Lemke P, et al., eds. *The Freshwater Budget of the Arctic Ocean*. Netherlands: Springer, 91–106
- Chen Min, Huang Yipu, Jin Mingming, et al. 2003. The sources of the upper and lower halocline water in the Canada Basin derived from isotopic tracers. *Sci China Series D Earth Sci*, 46(6): 625–639
- Cooper L W, Benner R, McClelland J W, et al. 2005. Linkages among runoff, dissolved organic carbon, and the stable oxygen isotope composition of seawater and other water mass indicators in the Arctic Ocean. *J Geophys Res*, 110(G2): G02013
- Cooper L W, McClelland J W, Holmes R M, et al. 2008. Flow-weighted values of runoff tracers ($\delta^{18}\text{O}$, DOC, Ba, alkalinity) from the six largest Arctic rivers. *Geophys Res Lett*, 35(18): L18606
- Cooper L W, Whitley T E, Grebmeier J M, et al. 1997. The nutrient, salinity, and stable oxygen isotope composition of Bering and Chukchi Seas waters in and near the Bering Strait. *J Geophys Res*, 102(C6): 12563–12573
- Coplen T B, Kendall C. 2000. Stable isotope and oxygen isotope ratios for selected sites of the US Geological Survey's NASQAN and Benchmark surface-water networks. US Geological Survey Open-File Report 00-160, 409
- Eicken H, Krouse H R, Kadko D, et al. 2002. Tracer studies of pathways and rates of meltwater transport through Arctic summer sea ice. *J Geophys Res*, 107(C10): 8046
- Ekwurzel B, Schlosser P, Mortlock R A, et al. 2001. River runoff, sea ice meltwater, and Pacific water distribution and mean residence times in the Arctic Ocean. *J Geophys Res*, 106(C5): 9075–9092
- Giles K A, Laxon S W, Ridout A L, et al. 2012. Western Arctic Ocean freshwater storage increased by wind-driven spin-up of the Beaufort Gyre. *Nat Geosci*, 5(3): 194–197
- Grebmeier J M, Cooper L W, DeNiro M J. 1990. Oxygen isotopic composition of bottom seawater and tunicate cellulose used as indicators of water masses in the northern Bering and Chukchi Seas. *Limnol Oceanogr*, 35(5): 1182–1195
- Guay C K H, Falkner K K, Muench R D, et al. 2001. Wind-driven transport pathways for Eurasian Arctic river discharge. *J Geophys Res*, 106(C6): 11469–11480
- Holloway G, Wang Zeliang. 2009. Representing eddy stress in an Arctic Ocean model. *J Geophys Res*, 114(C6): C06020
- Horita J, Ueda A, Mizukami K, et al. 1989. Automatic δD and $\delta^{18}\text{O}$ analyses of multi-water samples using H_2 - and CO_2 -water equilibration methods with a common equilibration set-up. *Int J Rad Appl Instrum Part A Appl Rad Isot*, 40(9): 801–805
- Johnson M A, Polyakov I V. 2001. The Laptev Sea as a source for recent Arctic Ocean salinity changes. *Geophys Res Lett*, 28(10): 2017–2020
- Jones E P, Anderson L G. 1986. On the origin of the chemical properties of the arctic ocean halocline. *J Geophys Res*, 91(C9): 10759–10767
- Jones E P, Anderson L G, Jutterström S, et al. 2008. Pacific freshwater, river water and sea ice meltwater across Arctic Ocean basins: results from the 2005 Beringia Expedition. *J Geophys Res*, 113(C8): C08012
- Jones E P, Anderson L G, Swift J H. 1998. Distribution of atlantic and pacific waters in the upper Arctic ocean: implications for circulation. *Geophys Res Lett*, 25(6): 765–768
- Macdonald R W, McLaughlin F A, Carmack E C. 2002. Fresh water

- and its sources during the SHEBA drift in the Canada Basin of the Arctic Ocean. *Deep-Sea Res I*, 49(10): 1769–1785
- Macdonald R W, Paton D, Carmack E C, et al. 1995. The freshwater budget and under-ice spreading of Mackenzie River water in the Canadian Beaufort Sea based on salinity and $^{18}\text{O}/^{16}\text{O}$ measurements in water and ice. *J Geophys Res*, 100(C1): 895–920
- Melling H, Moore R M. 1995. Modification of halocline source waters during freezing on the Beaufort Sea shelf: evidence from oxygen isotopes and dissolved nutrients. *Cont Shelf Res*, 15(1): 89–113
- Morison J, Kwok R, Peralta-Ferriz C, et al. 2012. Changing Arctic Ocean freshwater pathways. *Nature*, 481(7379): 66–70
- Newton R, Schlosser P, Martinson D G, et al. 2008. Freshwater distribution in the Arctic Ocean: simulation with a high-resolution model and model-data comparison. *J Geophys Res*, 113(C5): C05024
- Newton R, Schlosser P, Mortlock R, et al. 2013. Canadian Basin freshwater sources and changes: Results from the 2005 Arctic Ocean Section. *J Geophys Res*, 118(4): 2133–2154
- Östlund H G, Hut G. 1984. Arctic Ocean water mass balance from isotope data. *J Geophys Res*, 89(C4): 6373–6382
- Pan Hong, Chen Min, Tong Jinlu, et al. 2015. Spatial and temporal variations of freshwater components at a transect near the Bering Strait during 2003–2012. *Haiyang Xuebao* (in Chinese), 37(11): 135–146
- Perovich D K, Richter-Menge J A, Jones K F, et al. 2011. Arctic sea-ice melt in 2008 and the role of solar heating. *Ann Glaciol*, 52(57): 355–359
- Pfirman S, Haxby W, Eicken H, et al. 2004. Drifting Arctic sea ice archives changes in ocean surface conditions. *Geophys Res Lett*, 31(19): L19401
- Pickart R S, Pratt L J, Torres D J, et al. 2010. Evolution and dynamics of the flow through Herald Canyon in the western Chukchi Sea. *Deep-Sea Research II*, 57(1–2): 5–26
- Proshutinsky A, Bourke R H, McLaughlin F A. 2002. The role of the Beaufort Gyre in Arctic climate variability: seasonal to decadal climate scales. *Geophys Res Lett*, 29(23): 15–1
- Proshutinsky A Y, Johnson M A. 1997. Two circulation regimes of the wind-driven Arctic Ocean. *J Geophys Res*, 102(C6): 12493–12514
- Proshutinsky A, Krishfield R, Timmermans M L, et al. 2009. Beaufort Gyre freshwater reservoir: state and variability from observations. *J Geophys Res*, 114: C00A10
- Rudels B, Anderson L G, Jones E P. 1996. Formation and evolution of the surface mixed layer and halocline of the Arctic Ocean. *J Geophys Res*, 101(C4): 8807–8821
- Semiletov I P, Savelieva N I, Weller G E, et al. 2000. The dispersion of Siberian river flows into coastal waters: meteorological, hydrological and hydrochemical aspects. In: Lewis E L, Jones E P, Lemke P, et al., eds. *The Freshwater Budget of the Arctic Ocean*. Netherlands: Springer, 323–366
- Shi Jiuxin, Cao Yong, Zhao Jinping, et al. 2005. Distribution of Pacific-origin water in the region of the Chukchi Plateau in the Arctic Ocean in the summer of 2003. *Acta Oceanol Sinica*, 24(6): 12–24
- Shimada K, Kamoshida T, Itoh M, et al. 2006. Pacific ocean inflow: influence on catastrophic reduction of sea ice cover in the Arctic Ocean. *Geophys Res Lett*, 33(8): L08605
- Steele M, Morison J, Ermold W, et al. 2004. Circulation of summer Pacific halocline water in the Arctic Ocean. *J Geophys Res*, 109(C2): C02027
- Thompson D W J, Wallace J M. 1998. The Arctic Oscillation signature in the wintertime geopotential height and temperature fields. *Geophys Res Lett*, 25(9): 1297–1300
- Tong Jinlu, Chen Min, Qiu Yusheng, et al. 2014. Contrasting patterns of river runoff and sea-ice melted water in the Canada Basin. *Acta Oceanol Sinica*, 33(6): 46–52
- Woodgate R A, Aagaard K. 2005. Revising the Bering Strait freshwater flux into the Arctic Ocean. *Geophys Res Lett*, 32(2): L02602
- Woodgate R A, Aagaard K, Weingartner T J. 2006. Interannual changes in the Bering Strait fluxes of volume, heat and freshwater between 1991 and 2004. *Geophys Res Lett*, 33(15): L15609
- Woodgate R A, Weingartner T J, Lindsay R. 2012. Observed increases in Bering Strait oceanic fluxes from the Pacific to the Arctic from 2001 to 2011 and their impacts on the Arctic Ocean water column. *Geophys Res Lett*, 39(24): L24603
- Yamamoto-Kawai M, Carmack E, McLaughlin F. 2006. Nitrogen balance and Arctic throughflow. *Nature*, 443(7107): 43
- Yamamoto-Kawai M, McLaughlin F A, Carmack E C, et al. 2008. Freshwater budget of the Canada Basin, Arctic Ocean, from salinity, $\delta^{18}\text{O}$, and nutrients. *J Geophys Res*, 113(C1): C01007
- Yamamoto-Kawai M, McLaughlin F A, Carmack E C, et al. 2009. Surface freshening of the Canada Basin, 2003–2007: river runoff versus sea ice meltwater. *J Geophys Res*, 114(C1): C00A05
- Yamamoto-Kawai M, Tanaka N, Pivovarov S. 2005. Freshwater and brine behaviors in the Arctic Ocean deduced from historical data of $\delta^{18}\text{O}$ and alkalinity (1929–2002 AD). *J Geophys Res*, 110(C10): C10003
- Zhao Jinping, Gao Guoping, Jiao Yutian. 2005. Warming in Arctic intermediate and deep waters around Chukchi Plateau and its adjacent regions in 1999. *Sci China Ser D: Earth Sci*, 48(8): 1312–1320